9.6   **NONSUPERCELL TROPICAL CYCLONE TORNADOES:**
DOCUMENTATION, CLASSIFICATION AND UNCERTAINTIES

Roger Edwards*, Andrew R. Dean, Richard L. Thompson and Bryan T. Smith
Storm Prediction Center, Norman, OK

1. INTRODUCTION and BACKGROUND

An ingredients-based approach (e.g., Johns and Doswell 1992) is used in the operational prediction of tornado threat, regardless of whether the favorable environment results from midlatitude or tropical perturbations. Since the majority of tropical cyclone (TC) tornadoes are associated with supercells (Edwards et al. 2012a; hereafter E12), the forecaster typically can focus on the same ingredients known to favor midlatitude supercells—moisture, instability, (sources for) lift, and vertical wind shear. As in midlatitude settings (e.g., Markowski et al. 1998; Garner 2012), supercellular tornado potential may be focused further by the presence of baroclinic and/or kinematic boundaries within the TC envelope (Edwards and Pietrycha 2006).

Still, TCs present a unique forecast setting for supercell tornadoes, in that they represent a physically distinct, spiral form of mesoscale convective system (MCS) with specific environmental characteristics (Edwards 2012). In a TC, the relative prevalence of the favorable ingredients for supercells is weighted heavily toward moisture and low-level vertical shear, each of which are usually abundant but still can be nonuniform (e.g., McCaul 1991; Curtis 2004; E12). In contrast, indicators of instability (lapse rates) and buoyancy (CAPE) may be either weak throughout or distributed with pronounced asymmetry away from center—typically downshear with respect to ambient midlatitude flow aloft (McCaul 1991; Verbout et al. 2007; Molinari and Vollaro 2010; E12). Boundaries can be well-defined or relatively subtle (Edwards and Pietrycha 2006; Green et al. 2011). Cumulative juxtaposition of those favorable foci yields a pronounced climatological tendency for TC tornadoes to occur generally north through southeast of center (e.g., Schultz and Cecil 2009, Edwards 2012).

Some TC tornadoes, however, are not associated with identifiable supercells, even in mesoscale environments that favor storm-scale rotation (E12 and section 3). Those are classified herein as non-supercell TC (NSTC) tornadoes, as in E12. Nonsupercell tornadoes in non-TC settings have been studied for over two decades (e.g., Wakimoto and Wilson 1989), but not explicitly examined in TCs until E12 and this more detailed work. We summarize and

expands upon E12 findings via analyses specific to NSTC tornadoes. Section 2 discusses the compilation of NSTC tornado records and potential sources for error, their occurrence relative to supercell tornadoes, and various measures of the spatial and temporal distribution of NSTC events. Section 3 offers distributive and environmental analyses of NSTC tornado events. Section 4 encapsulates our findings and presents discussion and recommendations.

2. DATA and CLASSIFICATIONS

a. Tornado data and filtering

For E12 and herein, all TC tornado events examined were taken from the Storm Prediction Center's tropical cyclone tornado dataset (TCTOR; Edwards 2010). Although TCTOR spans the era of full WSR-88D deployment within ~500 km of the Atlantic and Gulf coasts (1995–2011 as of this writing), gridded mesoscale environmental information used in Thompson et al. (2012), E12 and in section 3 is available only from 2003 onward. As such, TC tornado data came from that subset of TCTOR spanning 2003–2011.

The TCTOR data then were filtered on a gridded basis, as described in detail in Smith et al. (2012; hereafter S12). To summarize, it is not whole-tornado data. Instead, the 826 TCTOR records from 2003–2011 were segmented by county. Each filtered tornado record consists of the county-segment rated highest on the Fujita or enhanced Fujita (EF) damage scale (Doswell et al. 2009; Edwards et al. 2012b), in a 40-km grid square, within a whole environmental-analysis hour (section 2c). For example, if a tornado occurred over portions of two counties inside one grid box—one segment rated EF0, the other EF1—the start time and location of the EF1 segment were used. Any less-damaging tornado segments in the same hour and grid box were removed, even if occurring with separate whole-tornado paths. This process distilled 730 filtered tornado records, hereafter deemed "tornadoes" or "events" for brevity.

b. Convective mode via radar

Further segregation of tornadic convection into supercell, marginal supercell and nonsupercell bins was accomplished via examination of archived, volumetric radar reflectivity and velocity imagery for each event, based on the convective-mode grouping scheme of S12. Those primary categories were defined as follows, with sample sizes and percentages of the TC tornado total:

_____
* _Corresponding author address:_ Roger Edwards, Storm Prediction Center, National Weather Center, 120 Boren Blvd #2300, Norman, OK 73072; E-mail: roger.edwards@noaa.gov

• **Supercell:** Containing a deep, persistent mesocyclone with ≥10 m s^{-1} rotational velocity at most ranges (maximum during tornado lifespan)—no anticyclonic supercells found in TCs; 576 events (79%).
• **Marginal supercell:** Exhibiting some evidence of transient rotation at one or more volumetric beam tilts, but not meeting supercell criteria; 63 events (9%).
• **Nonsupercell:** All other velocity and reflectivity signatures associated with tornadoes, non-rotational or exhibiting weak, non-rotational, horizontal shear; 85 events (12%).

Six events out of 730 (<1%) were unclassified. In those cases, the tornadic storm was out of radar range or radar data were missing, but environmental analyses were performed for E12. These are not included in our analyses, yielding 724 total events.

Ten specific convective modes encompassing the above three bins were associated with TC tornadoes in E12. The following four were entirely nonsupercellular. Of these, 85 cases are examined herein, with sample sizes and percentages of the NSTC event total:

• **Discrete:** Separated from other cells at ≥35 dBZ; 13 events (15%), e.g., Fig. 1a–c.
• **Quasi-linear convective system (QLCS):** Conterminous reflectivities ≥35 dBZ over ≥100 km long-axis length, with ≥3 to 1 axial aspect ratio; included embedded cells; 21 events (25%), e.g., Fig. 1d–f.
• **Cluster:** Conterminous reflectivities ≥35 dBZ using < 3 to 1 axial aspect ratio; included diffuse and/or disorganized reflectivity patterns, eyewalls and eyewall remnants; 25 events (29%), e.g., Fig. 1g–i. Also known as "disorganized" (S12).
• **Cell in cluster:** ≥35 dBZ echo connected to others but with distinctive, persistent higher-reflectivity maxima; 26 events (31%), e.g., Fig. 1j–l.

Some relatively straightforward examples of each of these NSTC tornadic convective modes are shown in Fig. 1. Most cases in each modal bin were not as well-defined in reflectivity as those, whether at 0.5º or in higher beam elevations (not shown). In fact, subjectively evaluated modal definition tended to become more difficult with greater elevation above radar level[1] (ARL), typically because of the shallow nature of the most intense portions of the echoes. Furthermore, because of the great variation in radar appearance and echo morphology within each mode—especially for those that are clustered—*the examples In Fig. 1 should not be considered archetypal.* Because of their nonsupercellular nature, velocity and spectrum-width presentations for all but a few mesovortex-affiliated QLCS signatures

were diffuse and/or undistinguished with regard to others nearby (section 3b). Figure 1e–f offers a QLCS exception.

The QLCS mode included spiral bands meeting aforementioned aspect–ratio and length criteria, as well as those convective bands on the outer reaches of TC circulations moving with some component outward from center. Meng and Zhang (2012) found that 40% of Chinese TCs in 3 y contained QLCS modes, using somewhat similar Parker and Johnson (2000) criteria (conterminous reflectivities ≥40 dBZ over ≥100 km but for 3-h duration).

c. Environmental data

Gridded, hourly environmental data, as described in detail by Schneider and Dean (2008), were associated with each tornado in our analysis. If the time of the tornado record was 2155 UTC, it was assigned to the 2100 UTC analysis hour. In summary, the environmental dataset consists of objectively analyzed surface observations applied to a first-guess field composed of the hourly Rapid Update Cycle (RUC[2], after Benjamin et al. 2004) analysis. The surface field then is combined with RUC gridded data aloft, as with the hourly SPC mesoanalyses (Bothwell et al. 2002). The resulting three-dimensional data can be passed through a modern Linux version of the Skew-T Analysis and Hodograph Research Program (Hart and Korotky 1991) to yield numerous derived environmental parameters.

d. Possible causes of data error

Potential sources for error in the TC tornado, radar and environmental data are offered in E12. To summarize, these include:
- Time errors of reports not attributable to any collocated echo. Five NSTC events were corrected to the nearest echo time of passage over the report location. Two other reports could not be associated with a specific echo. A few other events *may have been* associated with a different, stronger echo than the spatially closest one at radar time, but in absence of substantial velocity signatures characteristic of supercells, a definite time change could not be made.
- As described in S12, convective mode sometimes could not be categorized cleanly, especially between cell-in-cluster, QLCS and clustered modes. Diffuse or amorphous NSTC reflectivity patterns not meeting cell-in-cluster, QLCS or discrete criteria specified above were assigned to the "cluster" bin, making the latter category something of a catch-all for otherwise unclassifiable echoes (e.g., Fig. 2).
- Uncertainties regarding representativeness of environmental information mined from RUC-modulated data at 40-km horizontal grid spacing;
- Uncertainties with radar sampling, especially near and past radii ~165 km (~90 nm) where

---

[1] This was true whether higher absolute elevation resulted from greater beam angle at closer radii, or lesser beam angle at greater radii. The average and median distances of NSTC tornadoes from closest radar locations were 79 and 72 km respectively, with extrema of 4 and 169 km.

[2] The RUC was replaced operationally in May 2012 by the Rapid Refresh (Benjamin et al. 2007), which has not been evaluated in the TC tornado setting.
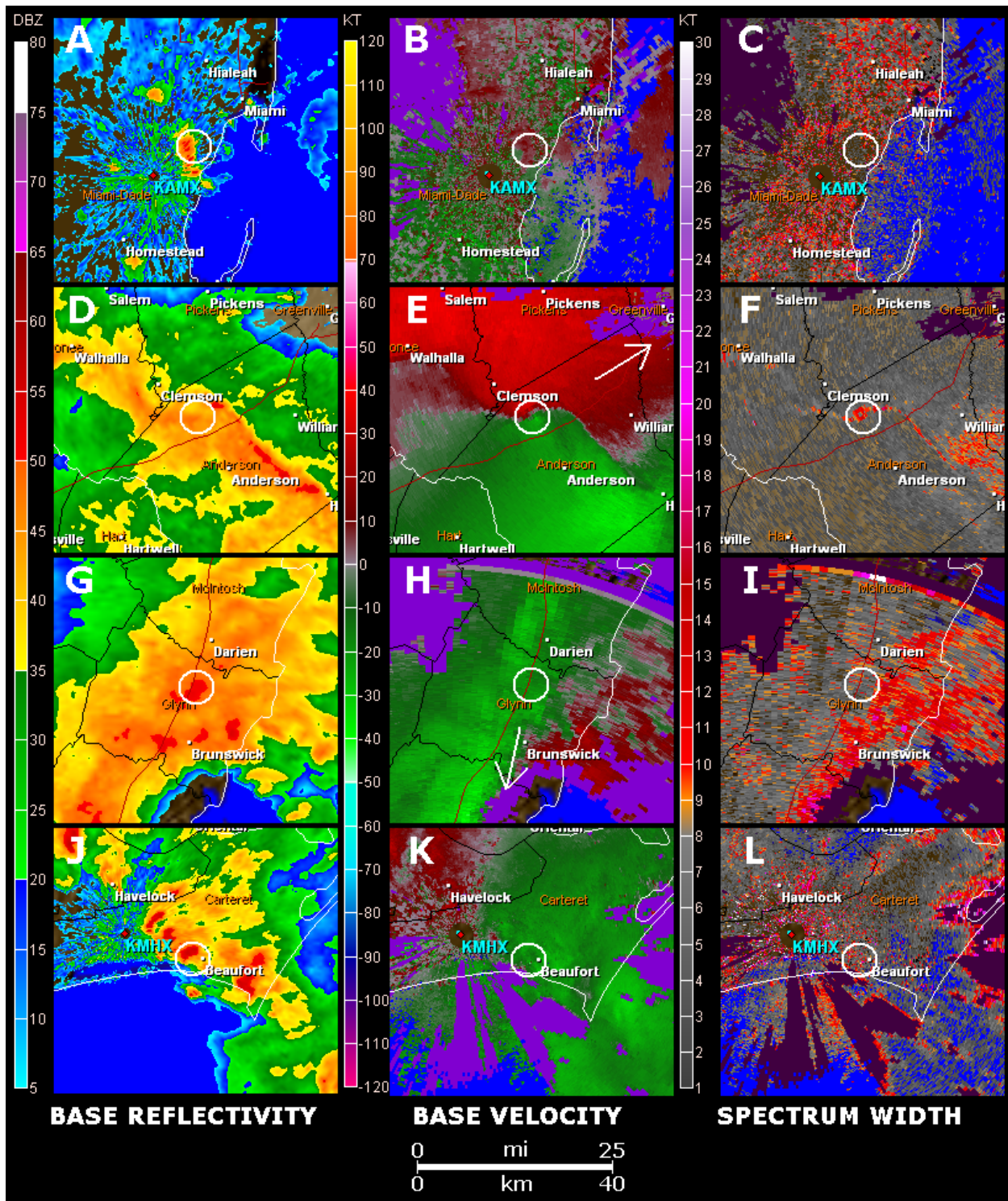
Figure 1: Radar imagery as labeled, 0.5º beam tilt. Panels represent the following convective modes, WSR-88Ds, times and contemporaneous TC classifications respectively: a–c) discrete, Miami, FL (KAMX), 1707 UTC 5 September 2003, Tropical Storm Henri; d–f) QLCS, Greer, SC (KGSP), 2338 UTC 7 September 2004, Tropical Depression Frances; g–i) cluster, Jacksonville, FL (KJAX), 0037 UTC 6 October 2005 (echoes in Georgia), Tropical Storm Tammy; j–l) cell in cluster, Morehead City, NC (KMHX), 1504 UTC 2 July 2003, Tropical Depression Bill. Circle encloses NSTC tornado location near time of image. Radar locations are red dots accompanied by cyan identifiers. Arrows on base velocity images (e) and (h) point toward off-map radars. Distance scale applies to all panels. County outlines in black, county names in orange. State boundaries, coastlines and municipality names in white. Color scale for moment magnitude is on left side of each column.
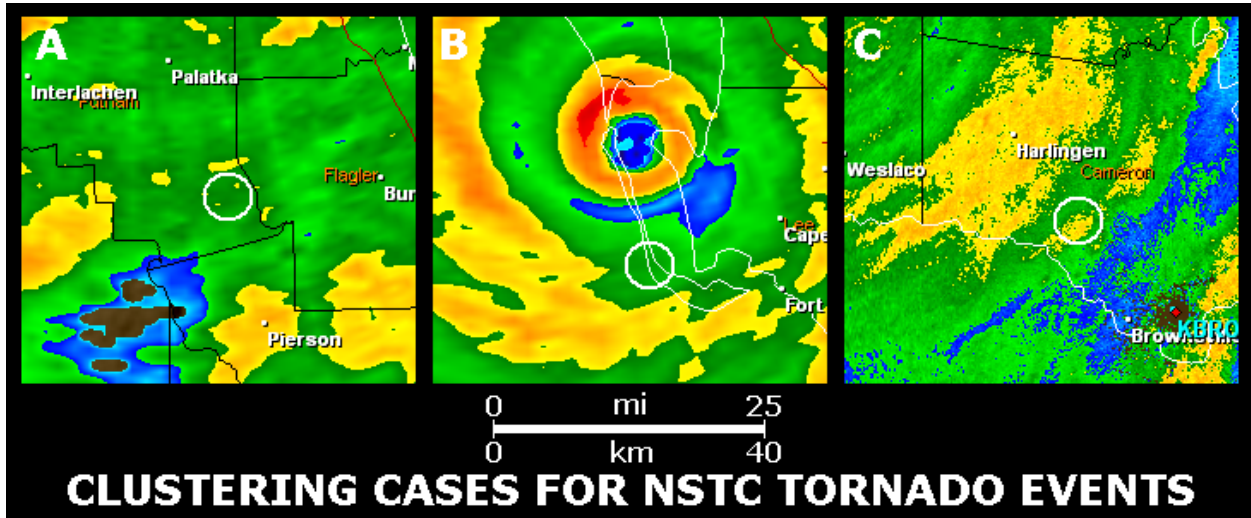
Figure 2: As in Fig. 1 reflectivity panels (a,d,g,j), except for cluster-mode NSTC tornado events sampled from: a) KJAX, 1915 UTC 5 September 2004, Tropical Storm Frances; b) Ruskin, FL (KTBW), 1956 UTC 13 August 2004, Hurricane Charley; c) Brownsville, TX (KBRO), 0405 UTC 24 July 2008, Hurricane Dolly.
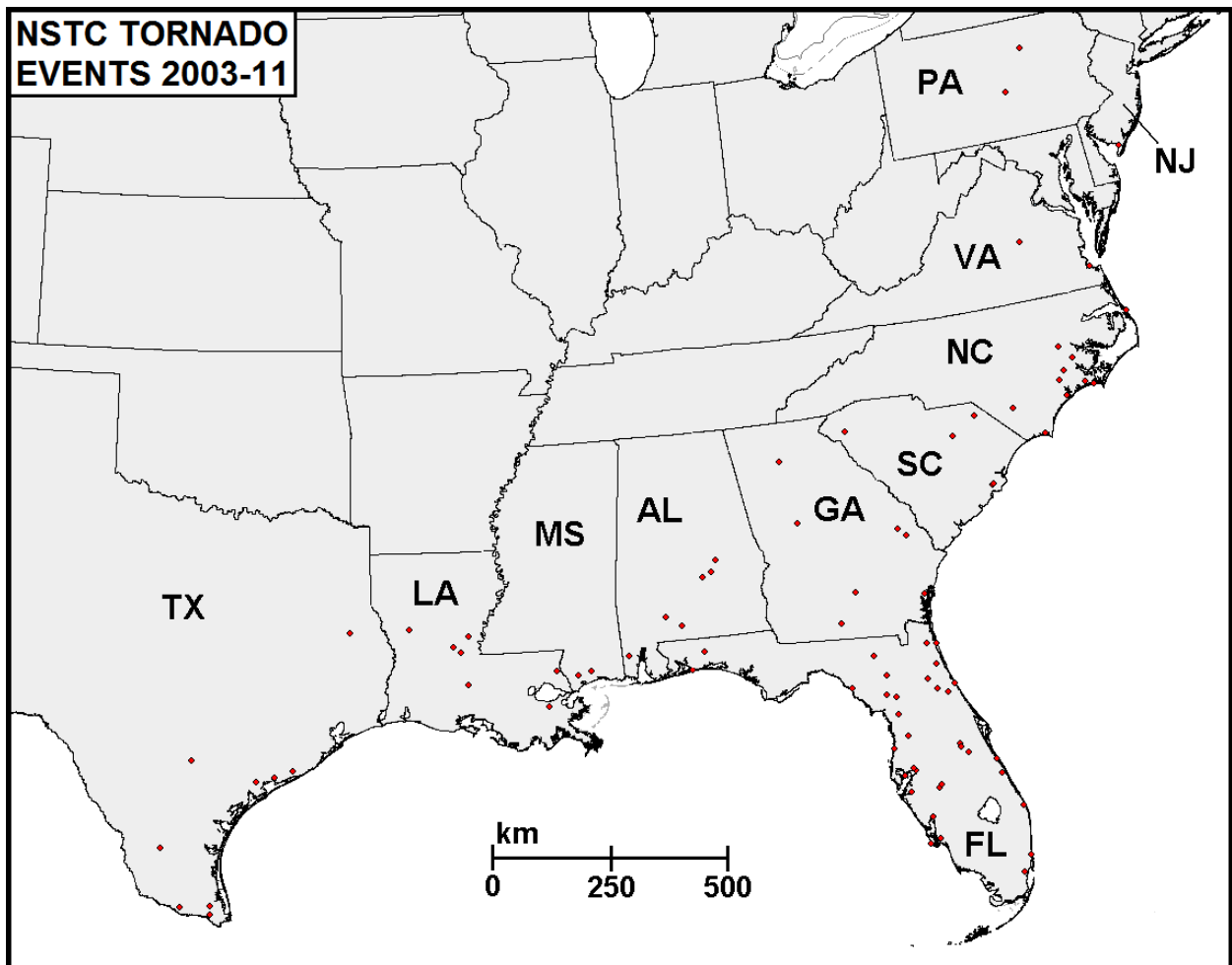

Figure 3: Geographic plot of NSTC tornado events (red) over the southern and eastern U. S., 2003–2011. States with tornadoes are labeled. Locations represent starts of segments used as tornado events, which are the same as tornadogenesis points in all but one case near the South Carolina coast. Dots may overlap where multiple events occurred. North points toward top of image parallel to eastern Texas border. Distance scale is true at 35° north latitude, or approximately the northern border of Mississippi, Alabama and Georgia.
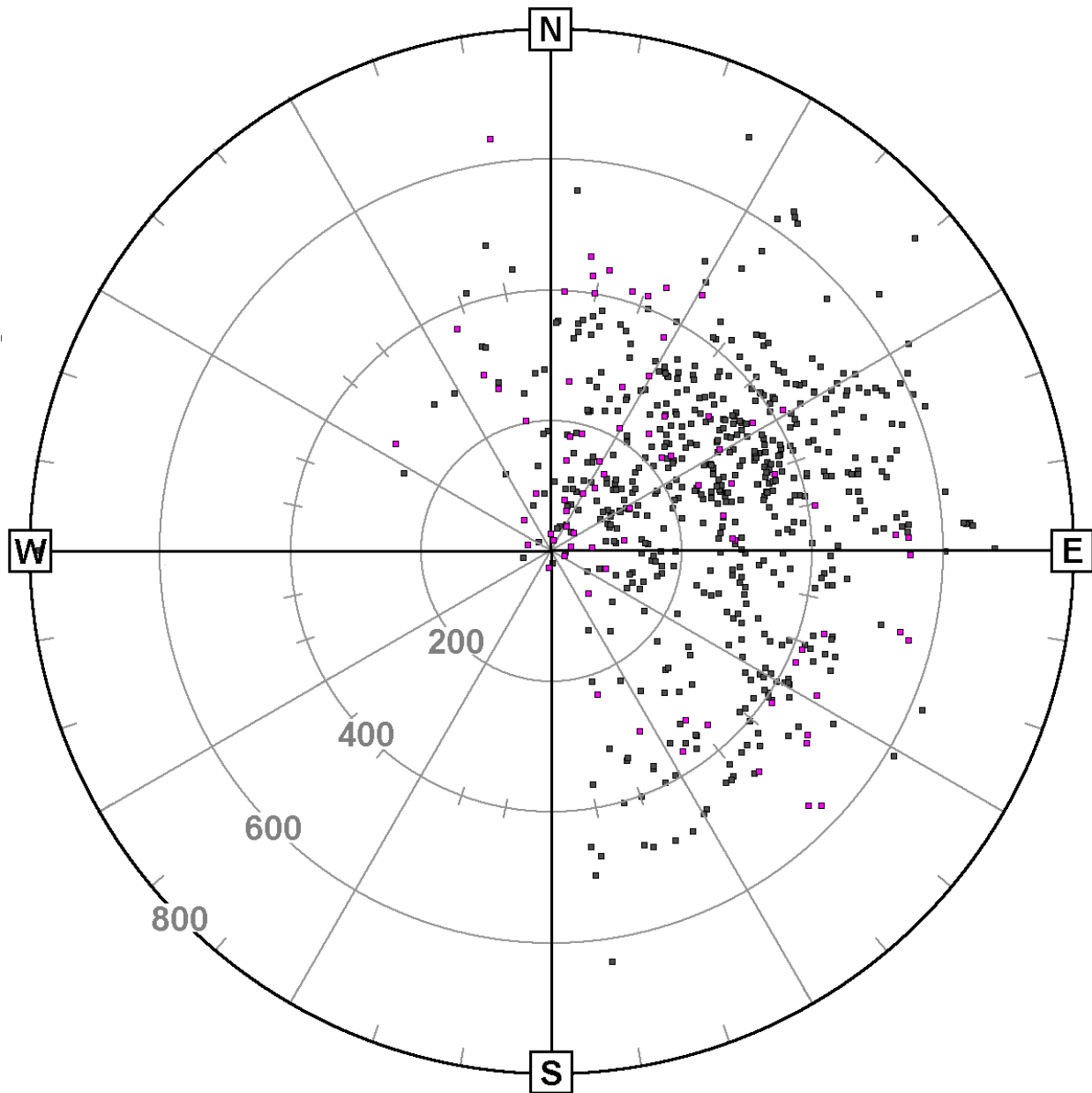
Figure 4: Polar plot of NSTC tornadoes (magenta) and supercell TC tornadoes from E12 (gray) relative to TC center, in a true-north framework. Radials every 30⁰. Range circles every 200 km as labeled. Marginal supercell events (E12) are not plotted.

beam height becomes ~3 km (~10 000 ft) ARL. Only two events were ≥150 km radius from their closest radars.

- Undetected tornadoes, which cannot be quantified;
- F/EF scale errors related to the subjectivity and inconsistency in damage rating (Doswell and Burgess 1988; Edwards et al. 2012b);
- Erroneous report types, which also are not quantifiable.

In the TCTOR era, NSTC tornado reports were justified in *Storm Data* based on either damage, eyewitness reports or no basis (i.e., no comments) at all. Photographic and video evidence of any of the NSTC tornadoes was not found. As such, it is possible that some fraction of them were mis-recorded as tornadoes, and instead would represent:

1) other forms of damage (e.g., from outflow winds, TC gusts or hydraulic effects), or 2) where no damage occurred, nontornadic cloud lowerings, or swirling ground-level eddies without physical continuity upward into the convective plume [e.g., Fujita (1993) "mini-swirls"]. Without any sort of confirming documentation beyond either hearsay reports or the presence of invariably weak (EF0–EF1) damage, the fraction of authentic NSTC tornado records is unknown.

3. ANALYSES

An order of magnitude fewer NSTC tornadoes were classified than those observed with supercells. The relatively small sample size (Doswell and Schultz 2006) of NSTC tornadoes, especially when broken down by convective mode, should be considered when evaluating any of the findings below.

a. Tornado occurrence

Geographically, NSTC tornadoes tended to occur within 500 km of the nearest seacoast (Fig. 3). Their concentration was more apparent near the Gulf of Mexico and Atlantic Ocean than for both the 1950–2007 TC tornado climatology (Fig. 4 in Schultz and Cecil 2009) and the 1995–2010 TCTOR dataset (Edwards 2012).

In TCTOR, center positions in the six-hourly National Hurricane Center TC-track data were interpolated to each tornado time. Center-relative positions for TCTOR events matching filtered tornadoes herein were plotted and compared to those for supercells, both graphically (Fig. 4) and analytically. NSTC (supercell) events averaged 302 (341) km from center, with respective medians of 287 (342) km (E12). In TCTOR, ≈30% of tornadoes associated with NSTC echoes occurred within 200 km of center, compared to ≈25% of all tornadoes (explicit radii for filtered supercell events are not tabulated yet). Based on examination of radar characteristics, the inward preference of NSTC tornadoes generally is attributed to their more common association with ill-defined and/or messy precipitation echoes closer to center (e.g., Fig. 2). These included diffuse banding features of weak reflectivity gradients as well as apparently weak-convective to nonconvective rain areas, each of which was placed in the clustered modal bin.

As with supercell tornadoes, times for NSTC events still showed a diurnal preference in an absolute sense (Fig. 5). A total of 54 (64%) occurred during the 1200–2359 UTC time frame, as compared to 72% of supercell events. This likely reflects the same diurnal-heating contribution to favorable low-level instability that aids potential for TC tornadoes as a whole (e.g., McCaul 1991), and the predominance of drying areas aloft (Curtis 2004) that contribute to destabilizing insolation in outer areas. Such effects are less pronounced with inward extent toward many TC centers, as the regime comes under the influence of: 1) central dense overcasts and 2) greater coverage of both convective and stratiform precipitation fields. Since NSTC tornadoes were somewhat more concentrated inward compared to those from supercells (Fig. 4), the contribution to their occurrence from diabatic surface destabilization should be lower. Indeed, Fig. 5 shows a greater tendency for NSTC tornadoes to occur nocturnally. These results are consistent with the overall tendency of TC tornadoes to occur closer to center at night while lessening in number (Fig. 7 in Edwards 2012).
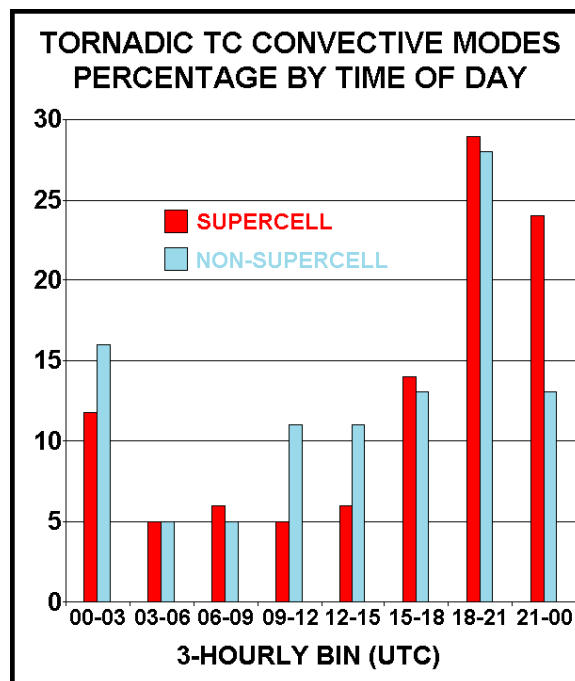

Figure 5: Bar chart of percentage (ordinate) and 3-hourly time range (abscissa) of supercell and NSTC tornadoes, as labeled. Tornadoes beginning at a time break were assigned to the start of that bin (i.e., 0300 UTC fell in the 03–06 bin). The 0000–1200 UTC bins include local nighttime.

Table 1: Fraction of 2003-2011 tornado damage rating occurrence for NSTC, supercell TC (STC) and non-TC (NTC) right-moving[3] supercells. Sample sizes are given in the top row.

Damage (F/EF)	NSTC 85	STC 576	NTC 12 560
≥4	.00	.00	.01
3	.00	.01	.05
2	.00	.08	.12
1	.20	.33	.30
0	.80	.58	.53

When comparing tornado origin from NSTC to TC supercell to non-TC, the damage ratings tended to weaken—quite markedly so for NSTC events. Table 1 summarizes the results from S12 and the subset examined herein. NSTC tornadoes from all storm modes were weak; no significant (≥EF2 rated) NSTC tornadoes occurred. This compares to 54 significant supercell TC tornadoes from E12, which represents 9% of tornadoes from TC supercells. Except for the lack of significant (≥EF2) damage with NSTC events, *these results should not be interpreted to apply to actual (non-filtered) tornadoes!* This is because maximum rating was used as a grid filter. Therefore, the literal fractions of strong to weak tornadoes of all origins, and of EF1 to EF0 NSTC events, are lower than in our analyses.

---

[3] Only right-moving non-TC supercells are compared, since no left-movers were found in TCs.

b. Storm-mode characteristics

The greatest variability in radar characteristics such as echo geometry, base-moment intensity and morphology were evident within the cluster category—the one commonality to all cases being the lack of either strength or continuity to any particular velocity or spectrum width signature.

In contrast, four (19% of) QLCS events showed unambiguous mesocirculations—for this purpose, persistent horizontal cyclonic shear at more than one elevation angle, and appearing in multiple volume scans. The QLCS example in Fig. 1 was the most pronounced of this sort. Six (29%) QLCS events exhibited weak and/or transient cyclonic shear near tornado time and location. For the balance, where weak horizontal changes in velocity or spectrum width were evident at or near the time and location of a tornado report, these signatures were not visibly different from those occurring elsewhere in the region—often in nontornadic locales and echo types. Clustered modes universally offered signatures of reflectivity (e.g., Fig. 2), base velocity (e.g., Fig. 1h,k) and spectrum width (e.g., Fig. 1i,l) that did not appear substantially distinguishable from those in nontornadic areas of the same TC at about the same time, whether analyzing a single frame or animating multiple frames.

Spectrum width, which was not examined in S12 or E12, has shown operational utility in diagnosing storm-scale areas of enhanced horizontal shear, mesovortices, tornadic circulations and small boundaries (Spoden et al. 2012)—especially with close proximity to a WSR-88D. One hypothesis of this study was that spectrum width should offer standout signatures for NSTC tornadoes, as it has for some nonsupercell tornado events in midlatitude settings. Still, except for some QLCS cases (the most prominent being Fig. 1f), coherent signatures were lacking. For non-QLCS modes, no consistent trends appeared regarding whether NSTC tornadoes were collocated with relative maxima or minima in spectrum width. We do not know the extent to which this antihypothetical finding is a function of either 1) imprecision in radar-data resolution for storm-scale NSTC tornado settings, or 2) inaccuracies that may remain in time or location of the events, per error sources given in section 2d.

Storm modes for NSTC tornadoes also were examined for predominance by time of day. The temporal distribution of largely diurnal (1200–2359 UTC) versus nocturnal (0000–1200 UTC) tornadoes fell roughly on a 2:1 ratio for all but the discrete mode, which had a diurnal tornado rate of only 46%. Small sample-size (i.e., 13 events) caveats apply; so it is probably too speculative at this time to interpret any physical meaning to the fact that a slight majority of discrete-mode NSTC tornadoes happened from 0000–1159 UTC.

c. Environmental parameters and convective depth

The full set of parameters analyzed in E12 also was examined for this study, with an emphasis on segregating NSTC events for comparison with fully supercell cases (e.g., Figs. 6 and 7). In order to maintain optimal sample size, statistical distributions were performed for thermodynamic computations resulting from fixed-layer rather than effective-layer (Thompson et al. 2007) methods, given the missing-data limitations described in more detail in S12 and E12. For NSTC data, sample size for most effective-parcel variables, and by extension, derived parameters such as supercell composite and significant tornado parameters (SCP and STP, respectively; Thompson et al. 2003) was in the low 30s, slightly over 1/3 of the total NSTC sample size, and too small for meaningful percentile examination after breaking it down into specific modes. As such, we compared the percentile distributions of fixed-layer variables and parameters to those in a larger (576-member[4]) TC supercell set.

Most parameters showed little distinction between NSTC and supercell classes (e.g., Fig. 6). A consistent tendency appeared for visually apparent but statistically insignificant underlay on low-level CAPE, as well as most shear-and helicity-related NSTC tornado distributions. The latter resulted in similar distinction for fixed-layer STP (Fig. 6d). The extent to which the considerable *spatial* overlap of supercell and NSTC events (Fig. 4) contributes to the *statistical* overlap is unknown and difficult to quantify, but we speculate that it is a nontrivial factor.

Nonetheless, and surprisingly, 0–3 and 0–6 km measures of fixed-layer bulk wind difference (BWD, Fig. 7) did distinguish supercell versus NSTC events. The latter represented the most prominent distinction among any variable or parameter (Fig. 7b). The 25th percentile for supercell TC events matched the 75th percentile for NSTC tornadoes; and the 90th percentile for NSTC tornadoes fell below the 50th percentile for those with supercells. A general tendency has been found for vertical *shear* in hurricanes to decrease with inward extent toward the radius of maximum wind, even though *speeds* increase (McCaul 1991; Molinari and Vollaro 2010). Imagery presented by Franklin et al. (2003) showed a general tendency for 0–3 km AGL BWD to increase outward from the eyewalls of hurricanes, except for a limited sampling of events with max surface winds >60 m s^{-1}. The tendency for NSTCs to occur closer to center, therefore, appears generally consistent with their relationship to weaker bulk shear. The 0–6 km layer lies above the Franklin et al. (2003) dropwindsonde data, and also *can* overshoot TC convection.

Given this unexpected finding, it is worth investigating the depth of NSTC tornadic storms. To gauge the relationship between that fixed 0–6 km layer and the NSTC cases, echo tops were estimated. Reflectivities >35 dBZ commonly are used to track initiation and progress of cumulonimbi from a nowcasting perspective (e.g., Mueller et al. 2003; Roberts and Rutledge 2003). However, some tornadic echoes in our dataset were associated with weaker reflectivities throughout their depths. As such,

---

[4] Individual missing data points account for totals <576 in sample sizes for calculations and figures herein.
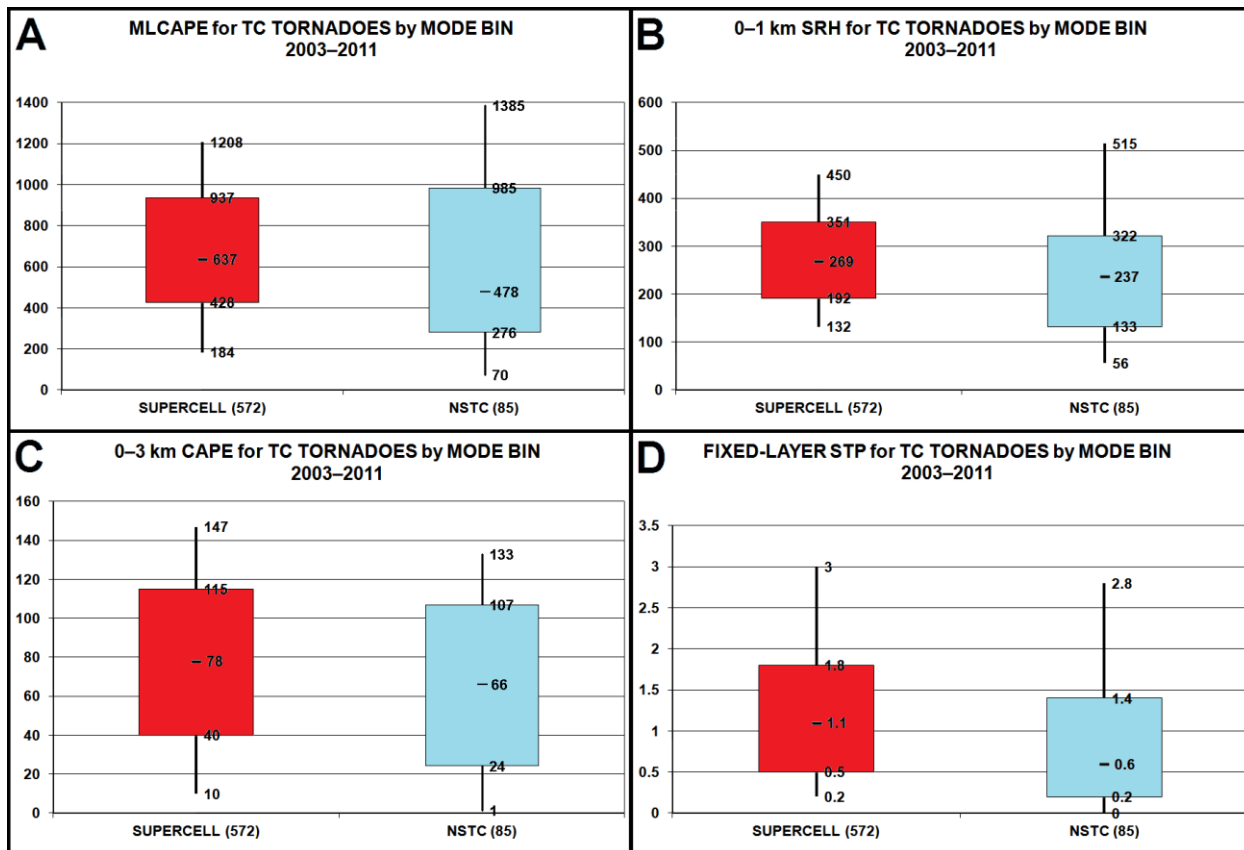
Figure 6: Box-and-whisker diagrams of environmental parameters for TC tornado categories as labeled, for: a) 100-mb mixed-layer CAPE (J kg^{-1}), b) 0–1-km AGL storm-relative helicity (m^2 s^{-2}), c) 0–3-km AGL CAPE (J kg^{-1}), and fixed-layer significant tornado parameter (unitless). Boxes represent middle 50% of distributions, while whiskers extend to 10th and 90th percentiles, values labeled. Medians correspond to labeled bars within each box.
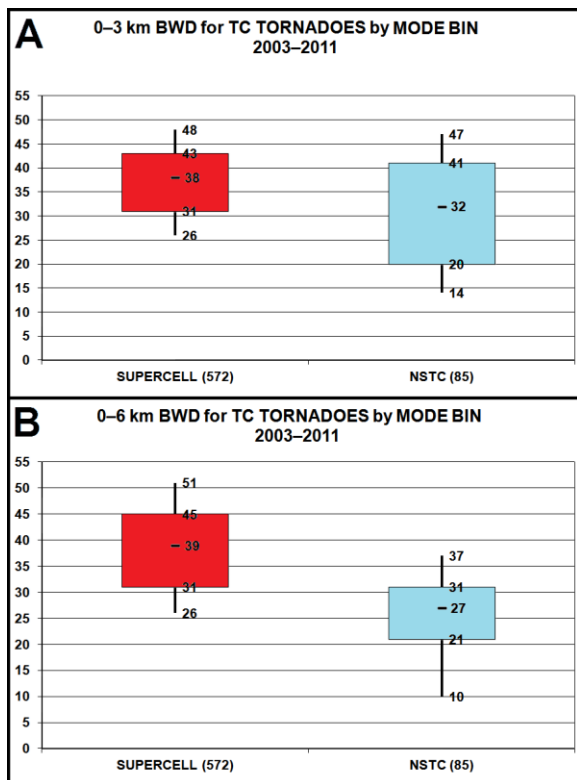

Figure 7 (left): As in Fig. 6, but for bulk wind difference (kt) through these layers AGL: a) 0–3 and b) 0–6 km.

we used three-dimensional (x,y,z) isosurfaces and interactively movable cross-sections to estimate the highest level of manually inspected 20-dBZ[5] values with associated echoes. This denoted "echo top" for NSTC tornado events is consistent with the tropical-convective criteria of Cifelli et al. (2007). Estimates could be made for 75 cases (88% of total). We have not investigated this yet for supercell TC tornadoes.

A few potential sources of inaccuracy and error exist with this approach, including:
- Uncertainties of tornado time vs. report location, which lead to substantial changes in the shape and max height of the 20-db$Z$ isosurface used as basis for the estimate if either the tornado time is off by as little as one volume scan;
- Changes in echo character and position within a scan—a definite concern for fast-moving cells;

---

[5] Other "echo top" heights in use include 18.5 dBZ for the GRLevelX™ default and 18 dBZ (Lakshmanan et al. 2012). The Storm Cell Identification and Tracking Algorithm (Johnson et al. 1998) begins with values of 30 dBZ. None of those are devoted specifically to tropical convection.

8

- Variations in isosurface height within a given echo—max was used when echo was over report location;
- Beam-size expansion at far distance, leading to resolution uncertainties, each estimate being assigned to a level in the middle of the beam;
- Vertical truncation of echoes located close to the nearest radar, in which case the data weren't used.

Given those uncertainties, echo-top estimates in the dataset were rounded to the nearest 1000 ft (305 m); and that still may be too precise.

Figure 8 shows the distribution of estimated echo tops with respect to the 0–6 km layer[6]. The median, mean (7.7 km, not shown) and middle 50% of the distribution exceeded 6 km, though slightly <1/4 (22%) of cases did not. The outlier echoes (not shown) were 2.7 and 15.2 km AGL. These findings indicate that 1) most NSTC tornado events are covered by fixed-layer 0-6 km sampling, and 2) there *may* be a physical, storm-scale basis for the statistical distinction (Fig. 7) between 6-km BWD for supercell and NSTC tornado events, pending echo-top work on the much larger supercellular dataset.

Echo tops at 20 dBZ were available for 20 QLCS, 21 cluster, 12 discrete, and 22 cell-in-cluster events. Their means, respectively, were 8.2, 7.7, 8.1 and 7.0 km. Caveats regarding small sample size clearly apply here; but preliminary results indicate NSTC QLCS events are deepest, cell-in-cluster events shallowest, and the majority of each reach >6 km AGL. Ideally, effective-layer measures of BWD render the fixed-layer overshooting problem moot, by the nature of the former's direct reliance on case-by-case CAPE depth as a proxy for storm depth (Thompson et al. 2007). However, the number of effective-layer NSTC events remains low at this time, and fixed-layer measures still are used commonly in operations.

Because of the small sample sizes of individual storm-mode bins, percentile analyses may not be adequately representative of actual relative distributions of environmental parameters. Some rough comparisons by mean and median are offered, however, in Table 2. The most prominent distinctions appeared in deep-shear measures, including small sample-size bins of effective BWD (Thompson et al. 2007). This is consistent with the substantial differences apparent in aforementioned distributive analyses of deeper fixed-layer indicators of shear (BWD). Effective storm-relative helicity (ESRH) and effective supercell composite parameter (ESCP) also showed some potential distinguishing utility (again, with a small sample-size caveat). Average (median) SRH for NSTC tornadoes was 73% (63%) of the value for supercell events; while ESCP was 64% (28%) of that for supercell tornadoes.
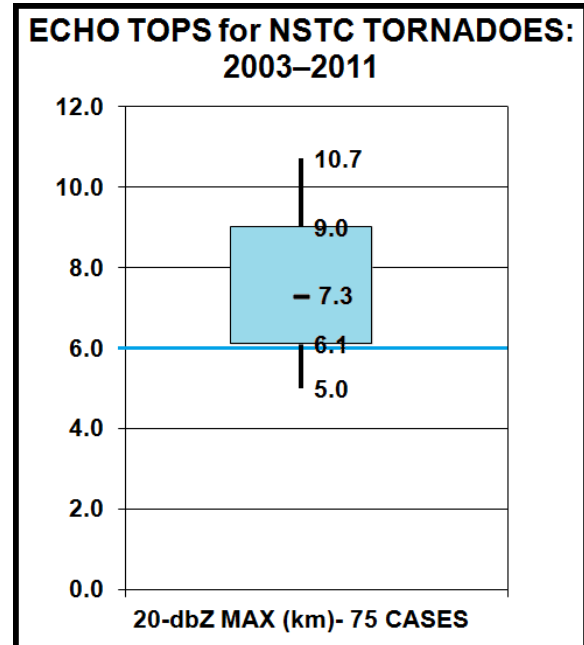

Figure 8: As in Fig. 6, but for 20-dBZ echo tops (km) for 75 NSTC tornado cases for which such data were available. 6-km level is highlighted in blue.

Table 2: Mean (median) values of parameters across the NSTC and supercell TC (STC) sets, in operationally common units. ML stands for 100-hPa mixed-layer parcels.

PARAMETER (units)	NSTC ≤85	STC ≤576
MLCAPE (J kg^{-1})	632 (478)	620 (544)
MUCAPE (J kg^{-1})	1249 (1177)	1337 (1254)
MLLCL (m)	695 (663)	727 (675)
0–3 km CAPE (J kg^{-1})	70 (66)	80 (78)
DCAPE* (J kg^{-1})	395 (351)	422 (411)
PRECIPITABLE WATER (in)	2.2 (2.2)	2.2 (2.2)
0–6 km BWD (kt)	30 (29)	38 (40)
0–3 km BWD (kt)	31 (32)	37 (38)
0–1 km BWD (kt)	29 (29)	31 (30)
EFFECTIVE^ BWD (kt)	27 (29)	38 (40)
0–3 km SRH (m^2 s^{-2})	307 (279)	351 (343)
0–1 km SRH (m^2 s^{-2})	257 (237)	281 (269)
EFFECTIVE^ SRH (m^2 s^{-2})	180 (140)	246 (223)
EFFECTIVE^ SCP	3.4 (1.3)	5.3 (4.7)
FIXED STP	1.0 (0.6)	1.4 (1.1)

* Downdraft CAPE (Gilmore and Wicker 1998)
^ 32-member sample size for NSTC events

---

[6] Radar data were sampled ARL instead of AGL, but that is a negligible difference on this scale.

The low relative mean and median for ESCP are influenced by the presence of ten null values (out of 32 total) in the NSTC dataset for this parameter. Weaker shear in the inner portions of TCs, relative to outer sectors where supercell tornadoes are more common, may influence these tendencies. In contrast, means and medians of most other NSTC tornado parameters were comparable or slightly less than those for supercell-tornado environments in TCs.

A few standout means and medians were evident in comparing environmental parameters for individual NSTC convective modes. QLCS events exhibited an average mixed-layer (ML) level of free convection (LFC) of 3.1 km, compared to 1.5, 1.2 and 2.1 km for the cluster, discrete, and cell-in-cluster modes respectively. . Similar tendencies were not evident in ML lifted condensation levels (LCLs), but did appear in most-unstable (MU) parcel LFC *and* LCL. QLCS events, however, did not stand out in terms of *median* values for LCL and LFC measures. Precipitable water (PW) values also did not stand out for QLCS, nor for any other modes. One hypothesis for this would be that the tendency of QLCS events to occur in outer reaches of TCs, relative to other modes, may influence their generally higher LFCs via larger surface dew-point depressions (i.e., lower near-surface RH) compared to the core regions of TCs, even as total moisture content (indicated via PW) varies little. That idea is not supported by the data, however, which shows that surface RH and dew points in the environmental dataset were not lowest for QLCSs—but instead, for discrete and cell-in-cluster modes, respectively. One exception to the higher QLCS values in LCL and LFC heights was with MLLCL values, whose means were maximized for discrete modes (845 m). All other modes had mean MLLCL <700 m, consistent with the typically moist TC setting.

Other outstanding parameters within NSTC tornadoes involved assorted CAPE measures and the clustered mode. For example, 0–3 km CAPE for clusters had an average (median) of 84 (86) J kg^{-1}, whereas the other modes were maximized at roughly 67 J kg^{-1}. Clustered modes similarly stood out in medians and means of MU, ML and surface-based CAPE. The finding of somewhat higher CAPE for clusters also is antihypothetical, considering the messy character of this mode.

4. DISCUSSION

In the period of this study, 85 (12%) TC tornado events did not occur with identifiable supercells. These were considered NSTC tornadoes, and could be associated with any of four radar-based convective modes. Regardless of distance from radar, these events failed to exhibit the Smith et al. (2012) shear and reflectivity characteristics for supercells. Indeed, except for a few events associated with convective-scale horizontal-shear signatures in QLCS modes, NSTC tornadoes typically were associated with ill-defined signatures in all three base radar moments. One of the major uncertainties involved in such data is in the veracity of NSTC tornado reports, especially in light of 1) their unfailingly weak (EF0–EF1)

damage, often consistent with ambient TC wind speeds, 2) lack of standout radar characteristics at the time and location of reports, and 3) absence of tangible authentication of their occurrence, aside from the secondhand reports that are sourced in *Storm Data*.

Independent corroboration of NSTC tornadoes is lacking in the form of photos, video or other direct documentation—even more so than for supercell TC events. This is true not only for tornadoes in eyewalls and their remnants (discussed in Edwards 2012), but also the other NSTC tornadoes herein, as described in *Storm Data*. Actual visual documentation or mobile-radar confirmation of NSTC tornadoes may remain elusive in any systematic way, even for field programs or storm chasers targeting TCs, because of

- The brief, weak and small nature of these events,
- Their common occurrence with messy, precipitation-laden and often ill-defined echoes as discussed above,
- Their occurrence away from supercells that can be specifically identified on radar and targeted by nearby observers.

These factors lend a considerable element of low potential for their observation, even when intended.

Much work remains possible in assessing environmental factors for all TC tornado events as well, including NSTC tornadoes to the extent that they can be verified. Nationwide expansion of the SPC environmental dataset is planned to extend backward in time for effective-layer parameters for the whole period. This, along with accumulation of events from 2012 onward into the future, will boost sample sizes substantially for all parameters and TC tornado events. Additional environmental parameters also are likely to be involved in the national dataset, and by extension, the TC tornado analyses.

Simulations of non-supercell tornadoes (e.g., Lee and Wilhelmson 1997a,b; 2000) may be adaptable to the TC environment, especially for relatively well-defined, reproducible QLCS processes where small-scale, embedded circulations or misocyclones sometimes have been identified (e.g., Fig. 1e). Such modeling may help to assess the veracity of NSTC tornadoes and by numerically simulating the physical processes that might yield them for the various convective modes.

REFERENCES

Benjamin, S. G., and Coauthors, 2004: An hourly assimilation–forecast cycle: The RUC. *Mon. Wea. Rev.*, **132**, 495–518.

——, and Coauthors, 2007: From radar-enhanced RUC to the WRF-based Rapid Refresh. Preprints, *18th Conf. on Numerical Weather Prediction*, Park City, UT, Amer. Meteor. Soc., J3.4.

Bothwell, P. D., J. A. Hart, and R. L. Thompson, 2002: An integrated three-dimensional objective analysis scheme in use at the Storm Prediction Center. Preprints, *21st Conf. on Severe Local Storms*, San Antonio, TX, Amer. Meteor. Soc., J117–J120.

Cifelli, R., S. W. Nesbitt, S. A. Rutledge, W. A. Petersen, and S. Yuter, 2007: Radar characteristics of precipitation features in the EPIC and TEPPS regions of the east Pacific. *Mon. Wea. Rev.*, **135**, 1576–1595.

Curtis, L., 2004: Midlevel dry intrusions as a factor in tornado outbreaks associated with landfalling tropical cyclones from the Atlantic and Gulf of Mexico. *Wea. Forecasting*, **19**, 411–427.

Doswell, C. A. III, and D. W. Burgess, 1988: On some issues of United States tornado climatology. *Mon. Wea. Rev.*, **116**, 495–501.

——, and D. M. Schultz, 2006: On the use of indices and parameters in forecasting severe storms. *Electronic J. Severe Storms Meteor.*, **1** (3), 1–22.

——, C. A. III, H. E. Brooks, and N. Dotzek, 2009: On the implementation of the enhanced Fujita scale in the USA. *Atmos. Res.*, **93**, 554–563.

Edwards, R., 2010: Tropical cyclone tornado records for the modernized National Weather Service era. Preprints, *25th Conf. on Severe Local Storms*, Denver, CO, Amer. Meteor. Soc., P2.7.

——, 2012: Tropical cyclone tornadoes: A review of knowledge in research and prediction. *Electronic J. Severe Storms Meteor.*, **7** (6), 1-61.

——, and A. E. Pietrycha, 2006: Archetypes for surface baroclinic boundaries influencing tropical cyclone tornado occurrence. Preprints, *23rd Conf. on Severe Local Storms*, Saint Louis MO, Amer. Meteor. Soc., P8.2.

——, A. R. Dean, R. L. Thompson, and B. T. Smith, 2012a: Convective modes for significant severe thunderstorms in the contiguous United States. Part III: Tropical cyclone tornadoes. *Wea. Forecasting*, in press. doi: 10.1175/WAF-D-12-00084.1.

——, J. G. LaDue, J. T. Ferree, K. Scharfenberg, C. Maier, and W. L. Coulbourne, 2012b: Tornado intensity estimation: Past, present and future. *Bull. Amer. Meteor. Soc.*, in press. doi: 10.1175/BAMS-D-11-00006.

Franklin, J. L., M. L. Black, and K. Valde, 2003: GPS dropwindsonde wind profiles in hurricanes and their operational implications. *Wea. Forecasting*, **18**, 32–44.

Fujita, T. T., 1993: Damage survey of Hurricane Andrew in South Florida by Ted Fujita. *Storm Data*, **34** (8), 25–29. [Available from National Climatic Data Center, Asheville, NC, 28801.]

Garner, J. M., 2012: Environments of significant tornadoes occurring within the warm sector versus those occurring along surface baroclinic boundaries. *Electronic J. Severe Storms Meteor.*, **7** (5), 1–28.

Gilmore, M. S., and L. J. Wicker, 1998: The influence of midtropospheric dryness on supercell morphology and evolution. *Mon. Wea. Rev.*, **126**, 943–958.

Green, B. W., F. Zhang, and P. M. Markowski, 2011: Multiscale processes leading to supercells in the landfalling outer rainbands of Hurricane Katrina (2005). *Wea. Forecasting*, **26**, 828–847.

Hart, J. A., and W. Korotky, 1991: The SHARP workstation v1.50 users guide. National Weather Service, NOAA, U.S. Department of Commerce, 30 pp. [Available from NWS Eastern Region Headquarters, 630 Johnson Ave., Bohemia, NY 11716.]

Johns, R. H., and C. A. Doswell III, 1992: Severe local storms forecasting. *Wea. Forecasting*, **7**, 588–612.

Johnson, J. T., P. L. MacKeen, A. Witt, E. D. Mitchell, G. J. Stumpf, M. D. Eilts, and K. W. Thomas, 1998: The Storm Cell Identification and Tracking (SCIT) algorithm: An enhanced WSR-88D algorithm. *Wea. Forecasting*, **13,** 263–276.

Lakshmanan, V., K. Hondl, C. K. Potvin, and D. Preignitz, 2012: An improved method to estimate radar echo top height. *Wea. Forecasting*, in press. doi:10.1175/WAF-D-12-00084.1.

Lee, B. D., and R. B. Wilhelmson, 1997a: The numerical simulation of non-supercell tornadogenesis. Part I: Initiation and evolution of pre-tornadic misocyclone circulations along a dry outflow boundary. *J. Atmos. Sci.*, **54**, 32–60.

——, and ——, 1997b: The numerical simulation of non-supercell tornadogenesis. Part II: Evolution of a family of tornadoes along a weak outflow boundary. *J. Atmos. Sci.*, **54**, 2387–2415.

——, and ——, 2000: The numerical simulation of nonsupercell tornadogenesis. Part III: Parameter tests investigating the role of CAPE, vortex sheet strength, and boundary layer vertical shear. *J. Atmos. Sci.*, **57**, 2246–2261.

Markowski, P. M., E. N. Rasmussen, and J. M. Straka, 1998: The occurrence of tornadoes in supercells interacting with boundaries during VORTEX-95. *Wea. Forecasting*, **13**, 852–859.

McCaul, E. W. Jr., 1991: Buoyancy and shear characteristics of hurricane–tornado environments. *Mon. Wea. Rev.*, **119**, 1954–1978.

Meng, Z., and Y. Zhang, 2012: On the squall lines preceding landfalling tropical cyclones in China. *Mon. Wea. Rev.,* **140**, 445–470.

Molinari, J., and D. Vollaro, 2010: Distribution of helicity, CAPE, and shear in tropical cyclones. *J. Atmos. Sci.*, **67**, 274–284.

Mueller, C. K., T. Saxen, R. Roberts, J. Wilson, T. Betancourt, S. Dettling, N. Oien, and J. Yee, 2003: NCAR Auto-Nowcast system. *Wea. Forecasting*, **18**, 545–561.

Parker, M. D., and R. H. Johnson, 2000: Organizational modes of midlatitude mesoscale

convective systems. *Mon. Wea. Rev.*, **128**, 3413–3436.

Roberts, R. D., and S. Rutledge, 2003: Nowcasting storm initiation and growth using GOES-8 and WSR-88D data. *Wea. Forecasting*, **18**, 562–584.

Schultz, L. A., and D. J. Cecil, 2009: Tropical cyclone tornadoes, 1950–2007. *Mon. Wea. Rev.*, **137**, 3471–3484.

Schneider, R. S., and A. R. Dean, 2008: A Comprehensive 5-year severe storm environment climatology for the continental United States. Preprints, 24th Conf. on Severe Local Storms, Savannah GA, Amer. Meteor. Soc., 16A.4.

Smith, B. T., R. L. Thompson, J. S. Grams, C. Broyles, and H. E. Brooks, 2012: Convective modes for significant severe thunderstorms in the contiguous United States. Part I: Storm classification and climatology. *Wea. Forecasting*, **27**, 1136–1153.

Spoden, P. J., R. A. Wolf, and L. R. Lemon, 2012: Operational uses of spectrum width. *Electronic J. Severe Storms Meteor.,* **7** (2), 1–28.

Thompson, R. L., R. Edwards, J. A. Hart, K. L. Elmore, and P. Markowski, 2003: Close proximity soundings within supercell environments obtained from the Rapid Update Cycle. Wea. Forecasting, **18**, 1243–1261.

——, C. M. Mead, and R. Edwards, 2007: Effective storm-relative helicity and bulk shear in supercell thunderstorm environments. *Wea. Forecasting*, **22**, 102–115.

——, B. T. Smith, J. S. Grams, A. R. Dean, and C. Broyles, 2012: Convective modes for significant severe thunderstorms in the contiguous United States. Part II: Supercell and QLCS tornado environments climatology. *Wea. Forecasting*, **27**, 1136–1154.

Verbout, S. M., D. M. Schultz, L. M. Leslie, H. E. Brooks, D. J. Karoly and K. L. Elmore, 2007: Tornado outbreaks associated with landfalling hurricanes in the North Atlantic Basin: 1954–2004. *Meteor. Atmos. Phys.*, **97,** 255–271.

Wakimoto, R. M., and J. W. Wilson, 1989: Non-supercell tornadoes. *Mon. Wea. Rev.*, **117**, 1113–1140.